

1 **Sourcing the iron in the naturally-fertilised bloom around**  
2 **the Kerguelen Plateau: particulate trace metal dynamics**

3 **P. van der Merwe<sup>1</sup>, A. R. Bowie<sup>1,2</sup>, F. Qu  rou  <sup>1,2,3</sup>, L. Armand<sup>4</sup>, S. Blain<sup>5,6</sup>, F.**  
4 **Chever<sup>3,7</sup>, D. Davies<sup>1</sup>, F. Dehairs<sup>8</sup>, F. Planchon<sup>3</sup>, G. Sarthou<sup>9</sup>, A.T. Townsend<sup>10</sup>,**  
5 **T. W. Trull<sup>1,11</sup>**

6 [1]{Antarctic Climate and Ecosystems CRC, University of Tasmania, 7004, Australia}

7 [2]{Institute for Marine and Antarctic Studies, University of Tasmania, Battery Point, TAS  
8 7004, Australia}

9 [3]{Universit   de Brest, LEMAR, IUEM; Technop  le Brest Iroise, Place Nicolas Copernic,  
10 F-29280 Plouzan  , France}

11 [4]{Department of Biological Sciences and Climate Futures at Macquarie University, North  
12 Ryde, NSW 2109, Australia}

13 [5]{Sorbonne Universit  s, UPMC Univ Paris 06, UMR7621, Laboratoire d'Oc  anographie  
14 Microbienne, Observatoire Oc  anologique, 66650 Banyuls/mer, France}

15 [6]{CNRS, UMR7621, Laboratoire d'Oc  anographie Microbienne, Observatoire  
16 Oc  anologique, 66650 Banyuls/mer, France}

17 [7]{Ocean and Earth Science, National Oceanography Centre Southampton, University of  
18 Southampton, Southampton, SO14 3ZH, UK}

19 [8]{Vrije Universiteit Brussel, Analytical, Environmental and Geo-Chemistry & Earth System  
20 Sciences research group, Brussels, Belgium}

21 [9]{CNRS, Universit   de Brest, IRD, Ifremer, UMR 6539 LEMAR, IUEM ; Technop  le  
22 Brest Iroise, Place Nicolas Copernic, F-29280 Plouzan  , France}

23 [10]{Central Science Laboratory, University of Tasmania, Sandy Bay, TAS, 7005 Australia}

24 [11]{Commonwealth Scientific and Industrial Research Organisation, Oceans and Climate  
25 Flagship, GPO Box 1538, Hobart, Tasmania, Australia}

26 Correspondence to: P. van der Merwe (pvander@utas.edu.au)

27

## 1 **Abstract**

2 The KEOPS2 project aims to elucidate the role of natural Fe fertilisation on biogeochemical  
3 cycles and ecosystem functioning, including quantifying the sources and processes by which  
4 iron is delivered in the vicinity of the Kerguelen Archipelago, Southern Ocean. The KEOPS2  
5 process study used an upstream HNLC, deep water (2500 m), reference station to compare  
6 with a shallow (500 m), strongly fertilised plateau station and continued the observations to a  
7 downstream, bathymetrically trapped recirculation of the Polar Front where eddies commonly  
8 form and persist for hundreds of kilometres into the Southern Ocean. Over the Kerguelen  
9 Plateau, mean particulate (1-53  $\mu\text{m}$ ) Fe and Al concentrations ( $\text{pFe} = 13.4\text{nM}$ ,  $\text{pAl} = 25.2\text{ nM}$ )  
10 were more than 20-fold higher than at an offshore (lower-productivity) reference station ( $\text{pFe}$   
11  $= 0.53\text{ nM}$ ,  $\text{pAl} = 0.83\text{ nM}$ ). In comparison, over the plateau dissolved Fe levels were only  
12 elevated by a factor of  $\sim 2$ . Over the Kerguelen Plateau, ratios of  $\text{pMn/pAl}$  and  $\text{pFe/pAl}$   
13 resemble basalt, likely originating from glacial/fluviol inputs into shallow coastal waters. In  
14 downstream, offshore deep-waters, higher  $\text{pFe/pAl}$ , and  $\text{pMn/pAl}$  ratios were observed,  
15 suggesting loss of lithogenic material accompanied by retention of  $\text{pFe}$  and  $\text{pMn}$ . Biological  
16 uptake of dissolved Fe and Mn and conversion into the biogenic particulate fraction or  
17 aggregation of particulate metals onto bioaggregates also increased these ratios further in  
18 surface waters as the bloom developed within the recirculation structure. While resuspension  
19 of shelf sediments is likely to be one of the important mechanisms of Fe fertilisation over the  
20 plateau, fluvial and glacial sources appear to be important to areas downstream of the island.  
21 Vertical profiles within an offshore recirculation feature associated with the Polar Front show  
22  $\text{pFe}$  and  $\text{pMn}$  levels that were 6-fold and 3.5-fold lower respectively than over the plateau in  
23 surface waters, though still 3.6-fold and 1.7-fold higher respectively than the reference  
24 station. Within the recirculation feature, strong depletions of  $\text{pFe}$  and  $\text{pMn}$  were observed in  
25 the remnant winter water (temperature-minimum) layer near 175 m, with higher values above  
26 and below this depth. The correspondence between the  $\text{pFe}$  minima and the winter water  
27 temperature minima implies a seasonal cycle is involved in the supply of  $\text{pFe}$  into the  
28 fertilized region. This observed association is indicative of reduced supply in winter, which is  
29 counterintuitive if sediment resuspension and entrainment within the mixed layer is the  
30 primary fertilising mechanism to the downstream recirculation structure. Therefore, we  
31 hypothesise that lateral transport of  $\text{pFe}$  from shallow coastal waters is strong in spring,  
32 associated with snow melt and increased runoff due to rainfall, drawdown through summer

1 and reduced supply in winter when snowfall and freezing conditions predominate in the  
2 Kerguelen region.

### 3 **1 Introduction**

4 Small scale fertilisation experiments have now clearly established that Southern Ocean  
5 primary production is limited by the availability of the micronutrient iron (Fe) (Boyd et al.,  
6 2007; de Baar, 2005). This limitation on the biological pump means that the Southern Ocean  
7 does not realise its full potential in transferring atmospheric CO<sub>2</sub> into the ocean interior; a  
8 result illustrated in Antarctic continental ice records over geological timescales and supported  
9 by modelling studies (Barnola et al., 1987; Bopp et al., 2003; Martin, 1990; Watson et al.,  
10 2000). Less well understood is the overall system response to the addition of Fe as efficiency  
11 estimates (defined here as the amount of carbon exported relative to Fe added above baseline  
12 conditions) can vary by an order of magnitude (Blain et al., 2007; Pollard et al., 2009; Savoye  
13 et al., 2008). Both the original and subsequent KEOPS missions aimed to resolve not only the  
14 efficiency estimate, but also the response of the ecosystem and the overall effect on  
15 biogeochemical cycles due to natural Fe fertilisation in the vicinity of the Kerguelen plateau.  
16 The KEOPS natural fertilisation experiment is complementary to artificial Fe enrichment  
17 experiments due to the fact that its scale is much larger and timeframe longer than what is  
18 currently feasible in artificial fertilisation experiments. Furthermore, due to the sustained  
19 release of Fe into the fertilised region, as opposed to a sudden pulse artificial experiment, the  
20 technical challenges of monitoring carbon export are reduced. Furthermore, there is growing  
21 evidence that sustained Fe fertilisation favours large, highly silicified, slow growing diatoms  
22 that are efficient at exporting carbon into the ocean interior (Quéguiner, 2013). When the  
23 results of process studies such as KEOPS are extrapolated over the whole Southern Ocean, a  
24 small change in the efficiency estimate could result in different conclusions as to the efficacy,  
25 for instance, of artificial Fe fertilisation as a means of mitigating rising atmospheric  
26 concentrations of anthropogenic CO<sub>2</sub>.

27

28 Dissolved Fe (dFe < 0.2 µm) includes colloidal and nanoparticulate Fe, which may only be  
29 partially bioavailable, as well as soluble Fe (sFe < 0.02 µm) which is highly bioavailable (de  
30 Baar and de Jong, 2001). As a result, the larger particulate fraction (> 0.2 µm) is often less  
31 studied due to the perception that it has low bioavailability. However, the particulate fraction  
32 can yield important information for several reasons; firstly the dissolved fraction is constantly

1 in a state of change with uptake, particle scavenging and remineralisation occurring  
2 simultaneously and at varying rates depending on many factors including complexation with  
3 organic ligands (Johnson et al., 1997) and the biological community present (Sunda, 2001).  
4 Thus, interpretation of dFe data is difficult without a rarely-obtained perspective on the time  
5 varying aspects of the dFe distribution. Secondly, as a fraction of the total Fe, the major  
6 sources of Fe into fertilised regions (e.g. weathering products delivered by fluvial and glacial  
7 processes, resuspension of sediments and porewaters, atmospheric and extra-terrestrial dust)  
8 are small particles ( $> 0.2 \mu\text{m}$ ), with the concentration being more stable over weeks to  
9 months, due to its abundance and relatively slow biological uptake. The particulate fraction is  
10 primarily lost from surface waters through sinking, either directly or via adhesion to  
11 bioaggregates (Frew et al., 2006). However, there is a constant transfer of dissolved Fe to  
12 particulate Fe, either via biological uptake or precipitation and, particulate Fe to dissolved Fe,  
13 via dissolution and biologically mediated processes (Moffett, 2001). Thus, the particulate  
14 fraction that is small enough to avoid sinking out of the water column rapidly ( $0.2 - 5 \mu\text{m}$ ) can  
15 be considered as a significant source of dissolved Fe, with the rate of supply into surrounding  
16 waters dependent on the dissolution and leaching rate. Furthermore, there is growing  
17 evidence that particles in this size fraction are readily produced by mechanical erosion of  
18 bedrock due to glacial processes at high latitudes and that this large source may be partially  
19 bioavailable (Hawkings et al., 2014; Poulton and Raiswell, 2005; Raiswell et al., 2008a,  
20 2008b, 2006).

21

22 The first KEOPS process study was conducted in 2005 and specifically focused on processes  
23 affecting the demise of the Spring bloom over the Kerguelen Plateau (Blain et al., 2007).  
24 Blain et al., (2007) and Chever et al.,(2009) demonstrated that dFe fertilisation from the  
25 plateau increased primary production in the area. From the data gathered it was proposed that  
26 resuspension of plateau-derived sediments and entrainment into the mixed layer during  
27 increased wind mixing that deepened the mixed layer, was the primary source of particulate  
28 and subsequently, dissolved Fe to the downstream blooms. Resolution of the Fe budget  
29 (accounting for all sources and sinks of Fe in the system), from observations made during the  
30 first mission, found that the vertical supply of dissolved Fe was not sufficient to supply  
31 phytoplankton demand. Blain et al, (2007) closed the KEOPS Fe budget by assuming that  
32 dissolution of a small fraction of the unconstrained particulate Fe pool must occur. The

1 KEOPS2 mission aimed to improve on the successes of the first process study by accounting  
2 for the missing Fe in the budget, namely particulate Fe (pFe). Thus, we aim to test the  
3 KEOPS1 hypothesis that unconstrained particulate Fe is the missing Fe of the KEOPS Fe  
4 budget by documenting the particulate metal enrichment around the Kerguelen plateau. Our  
5 goal is to determine the sources of Fe enrichment within areas of interest (i.e. reference,  
6 plateau and the recirculation structure, see Fig. 1). Trace metal analysis of suspended  
7 particles, underlying sediment and settling particulate material will elucidate the source to  
8 sink progression of the particulate Fe pool. Following on from this work, and together with  
9 dissolved Fe measurements (Qu  rou   et al., 2015), a focused Fe budget will be constructed  
10 (Bowie et al., 2014).

## 11 **2 Methods**

### 12 **2.1 In situ pumps (ISP)**

13 All sample handling, processing and preparation was performed in accordance with general  
14 GEOTRACES protocols (<http://www.geotraces.org/>) and specific methodologies outlined in  
15 Bowie et al. (2010). Briefly, suspended particles were collected using up to 11 *in situ* pumps  
16 (ISPs) (McLane WTS and Challenger) suspended simultaneously at varying depths  
17 throughout the water column. Depths were chosen after viewing conductivity, temperature  
18 and depth (CTD) data to sample within oceanographic features of interest as well as obtaining  
19 a representative full water column profile. The ISPs were fitted with 142 mm quartz micro  
20 fibre (QMA) (Sartorius) filters with 53 µm Petex pre-filters and 350 µm polyester supports.  
21 QMA filters were pre-combusted to remove particulate organic carbon and then acid-washed  
22 with Seastar Baseline™ HCl and rinsed with copious amounts of ultra-pure water according  
23 to the methods outlined in the GEOTRACES sample handling protocols handbook (Cutter et  
24 al., 2010). The pre-filters and supports were carefully acid washed and rinsed with copious  
25 amounts of ultra-pure water before use. Both the Petex pre-filter and QMA filter were  
26 analysed for every pump giving two size fractions at each sampling location. Therefore, all  
27 particles greater than 53 µm were collected on the pre-filter and all particles within the 1 – 53  
28 µm size range were collected on the underlying QMA filter. Lithogenics sourced from  
29 bedrock or sediments in the larger size range (>53 µm) would have a high sinking velocity (>  
30 500 m day<sup>-1</sup>) according to Stokes law and as such would be expected to make up a relatively  
31 small fraction of the total particles in this size range. In comparison, the 1-53 µm size class  
32 can potentially capture both small biogenic and lithogenic particles. This is due to the

1 prediction that small lithogenic particles (1 – 5  $\mu\text{m}$ ) have significantly slower sinking rates  
2 (0.1 – 10  $\text{m day}^{-1}$ ) than large lithogenic particles according to Stokes law.

3 The ISPs were programmed to pump for up to four hours, allowing up to 2000 L of seawater  
4 to be filtered. After retrieval, the filters were bagged and processed within an ISO class 5,  
5 containerised clean room. Replicate 14 mm punches were taken using an acid-washed  
6 polycarbonate punch and stored frozen at  $-18\text{ }^{\circ}\text{C}$  until analysis at the home laboratory. The  
7 14 mm punches were then used for particulate metal analysis, particulate organic carbon and  
8 particulate organic nitrogen analysis.

9

## 10 **2.2 Sediment traps (Technicap PPS3)**

11 For a full description of the sediment trap data during KEOPS2 see Laurenceau et al. (2014)  
12 and Bowie et al. (2014). Two Technicap PPS3 free-floating sediment traps were deployed  
13 below the mixed layer at a depth of 200 m. The two sediment traps were deployed twice,  
14 giving a total of 4 deployments. The traps were prepared with acid-cleaned sampling cups  
15 containing low-trace-metal brine solution (salinity  $\sim 60$ ). The trap was programmed to sample  
16 for 1.5 to 5.5 days, whilst the 12 individual sampling containers were open for an equal  
17 portion of the total deployment. Upon retrieval, the sampling containers were removed from  
18 the carousel, sealed and processed within an ISO class 5, containerised clean room. The  
19 samples were filtered onto acid-washed, 2  $\mu\text{m}$  polycarbonate membrane filters via a 350  $\mu\text{m}$   
20 pre-filter using a Sartorius™ PTFE filtration unit. The 350  $\mu\text{m}$  pre-filter was selected to  
21 exclude large copepods and other large plankton that would lead to unrealistic sample  
22 variability.

23

## 24 **2.3 Sediment coring**

25 An Oktopus Multicorer ([www.oktopus-mari-tech.de](http://www.oktopus-mari-tech.de)) was used to collect 8 replicate, 610 x 95  
26 mm sediment cores, simultaneously within a  $1\text{ m}^2$  area at each station. The uppermost 5mm  
27 of surface sediment was subsampled according to Armand et al. (2008) representing an  
28 approximate sedimentation period of  $< 1000$  years.

29

## 1 **2.4 Analysis**

### 2 **2.4.1 ISP filters for particulate metals**

3 All digestions and evaporations were carried out within a digestion hood (SCP Science),  
4 where air was HEPA filtered during intake and subsequently extracted through a fume hood.  
5 Filter blanks and sample filters were digested in 15 mL acid cleaned, Teflon perfluoroalkoxy  
6 (PFA) screw cap vials (Savillex™) using ultra-pure nitric acid (1 mL 16 M HNO<sub>3</sub>) (Seastar  
7 Baseline™) heated to 120 °C for 12 hours on a Teflon coated hotplate (SCP Science  
8 DigiPREP™), following the method outlined in Bowie et al. (2010). Blanks containing only  
9 HNO<sub>3</sub> were also analysed to determine the contribution of the digestion acid without filter  
10 material.

11 The digest solution was diluted with 10 mL of ultra-high purity water and spiked with 10 ppb  
12 indium as an internal standard. Samples were analysed by Sector Field ICP-MS (Finnigan  
13 Element II, Thermo Scientific) (Cullen and Sherrell, 1999; Townsend, 2000). A full suite of  
14 trace elements was measured including Fe, Al, Mn, Ba, and P. The data were quality  
15 controlled by comparison with a certified reference material with a similar composition to the  
16 material collected (BCR-414 trace metals in phytoplankton, European Commission) (Table  
17 A1).

18 Quartz micro-fibre (QMA) filters were chosen as they could be acid cleaned to a trace-metal-  
19 clean level and the filter material allowed high particle loading and low wash-off upon pump  
20 retrieval. Furthermore, the filters were compatible for use with both Inductively Coupled  
21 Plasma Mass Spectrometry (ICP-MS) and elemental (CHN) analysis due to their ability to be  
22 combusted. It should be noted that a compromise was made here by using QMA filters on the  
23 ISPs. The compromise is that HF acid cannot be used with QMA filters as it digests the filter  
24 material completely and leads to unacceptably high analytical blanks. Therefore, we used  
25 HNO<sub>3</sub> for the digestions of the QMAs and for consistency regarding the suspended particles  
26 we also digested the pre-filter with the same acid. On the other hand, we used a full HF acid  
27 digestion for the underlying sediment analysis (Section 2.4.2). Therefore, recoveries of  
28 lithogenic trace elements will be close to 100% for the sediment analysis, but somewhat lower  
29 for the lithogenic suspended particles. However, a HNO<sub>3</sub> only digestion will recover  
30 effectively 100% of the trace elements of biogenic suspended particles (Table A1). For  
31 further information see Bowie et al., (Bowie et al., 2010).

## 1 2.4.2 Sediment analysis for particulate metals

2 Digestions and analysis were performed as per the ISP filters except that HF acid was used to  
3 digest these highly refractory samples. The HNO<sub>3</sub> digest used for the ISP filters is relatively  
4 weak but digests the biogenic fraction completely as evidenced by the excellent recoveries on  
5 the BCR414 certified reference material (trace metals in phytoplankton) (Table A1) but has  
6 limited recoveries of the lithogenic fraction as evidenced by the low recoveries of pAl and pTi  
7 in MESS-3 and PACS-2 sediment certified reference material (Bowie et al., 2010).

8 During the HF digest, a mixture of strong acids (250 µL HNO<sub>3</sub>, 250 µL HF and 500 µL HCl)  
9 were used as per Bowie et al. (Bowie et al., 2010). After 12 hours at 95° C the digest PFA  
10 vials were uncapped and evaporated to dryness under HEPA filtered air at 60° C for 4 hours.  
11 The digest was then resuspended in 10% HNO<sub>3</sub> with 10 ppb indium added as internal  
12 standard. A 100x dilution factor (v:v) was considered sufficient to place the ~20 mg sediment  
13 samples within the calibration range of the SF-ICP-MS.

14

## 15 2.4.3 Particulate organic carbon (POC) and nitrogen (PN)

16 All glassware in contact with POC samples was pre-combusted prior to field work (450 °C for  
17 12 h). Total nitrogen, carbon and hydrogen were determined at the Central Science  
18 Laboratory, University of Tasmania, using a Thermo Finnigan EA 1112 Series Flash  
19 Elemental Analyzer (estimated precision ~1%).

20

## 21 **3 Results and Discussion**

### 22 **3.1 Station-types**

23 The sampling locations of KEOPS2 (Fig. 1) were designed to capture the key regime types of  
24 the Kerguelen Archipelago including the high nutrient, low chlorophyll (HNLC) reference  
25 waters (station R-2), the high-trace-metal plateau waters (station A3), the northern Polar Front  
26 (station F-L) and a quasi-stationary, bathymetrically trapped recirculation structure (E-1, E-3  
27 and E-5) to the east of Kerguelen Island (Table 1). Stations E-1, E-3 and E-5 can be thought  
28 of as a pseudo-Lagrangian time series. In addition, two stations were sampled at the eastern



1 and western extremes of the recirculation structure (E-4W and E-4E) which proved to contrast  
2 in absolute concentrations as well as elemental ratios of particulate trace metals.

### 3 **3.2 Surface water flow around the Kerguelen Plateau**

4 During KEOPS1, van Beek et al. (2008), Zhang et al. (2008) and Chever et al. (2009)  
5 revealed that the water column southeast of Kerguelen Island was modified by passing over  
6 the Heard Island Plateau. Park et al. (2008) demonstrated that the interaction of the water  
7 masses over the Kerguelen Plateau could be divided into the southern and northern water  
8 masses separated by the Polar Front (PF) (Fig. 1). The southern water mass has source  
9 waters being derived from the Antarctic surface waters (AASW), southwest of Kerguelen  
10 which is bound to the north by the shallow bathymetry of the Leclaire Rise. These surface  
11 waters are generally colder and saltier than to the north (Fig. 2). The AASW also flows  
12 around Heard Island and a weaker surface current flows northwest over the Kerguelen Plateau  
13 towards the north east of Kerguelen Island where it is bound to the north by the PF. This cold  
14 surface current can be seen during winter in Figure 2. The northern water mass has a source  
15 of easterly flowing Sub Antarctic Surface Waters (SASW). The portion of the SASW that  
16 interacts with Kerguelen Island is termed Kerguelen Island source waters and is bound to the  
17 south by the PF (Fig. 2). A broad and poorly defined mixing zone to the east of Kerguelen  
18 Island has been identified at the junction of these southern and northern water masses. As a  
19 result of the mixing, eddies commonly form in this region. Also within this mixing zone,  
20 surface filaments, identified by elevated Chlorophyll *a*, can be seen in SeaWiFS images  
21 diverging from the PF and entering the eastern boundary of the recirculation structure (see  
22 supplementary material in Trull et al., (2014)).

23 The Kerguelen Archipelago is isolated, being a relatively small and localised source of Fe  
24 fertilisation surrounded by the large and deep, HNLC, low Fe, Southern Ocean. Therefore,  
25 when identifying an Fe source to the region, our focus is on the plateau and the two islands,  
26 Kerguelen and Heard. Over geological timescales, all pFe distributed throughout the water  
27 column within this region must be derived from all forms of weathering of bed rock  
28 including, fluvial and glacial outflow as well as dust from the islands, hydrothermal and extra-  
29 terrestrial input. Over shorter time frames, shelf sediments in the region contain recycled Fe  
30 as the vast majority of these sediments are a combination of siliceous ooze (Armand et al.,  
31 2008) and glacio-marine sediments; the exported product of the highly productive overlying  
32 waters together with some lithogenics (sourced from bed-rock) that were unutilised or non-

1 bioavailable and fast-sinking. Therefore, understanding the pathways of supply of this new  
2 Fe is important to understanding the processes controlling the long term productivity and  
3 therefore, carbon sequestration, in the area.

### 4 **3.3 Underlying sediment analysis**

5 Analysis of sediments sourced from cores taken at each station revealed a distinctly different  
6 sediment signature at station R-2 compared with any other station (Table 2). The reference  
7 station signature was approximately six times enriched in Mn relative to Al (Mn:Al 0.063) in  
8 comparison to the plateau station (A3) (Mn:Al 0.011). The Mn:Al sedimentary signature at  
9 A3 was almost identical to authigenic sediments previously reported from the Amundsen Sea  
10 (Angino, 1966). We consider the enriched Mn at R-2 could be due to either MnO<sub>2</sub> enrichment  
11 in the surface sediments during redox cycling of early diagenesis (Planquette et al., 2013), or  
12 supplied via a Mn enriched source such as hydrothermal venting near the Leclaire Rise. The  
13 extremely low carbon content of the sediment at station R-2, as evidenced by its near white  
14 colour, low diatom content (L. Armand, pers. obs.) and low carbon export flux (Laurenceau et  
15 al., 2014; Planchon et al., 2014), suggests that MnO<sub>2</sub> enrichment in the surface sediments  
16 during redox cycling is more likely at R-2.

17 The authigenic sediment ratio of Fe:Al was also lower at station R-2 (Fe:Al = 0.73) in  
18 comparison to any other station (Fe:Al range 0.81 – 1.1). However, all of our observed  
19 pFe:pAl molar ratios were higher than upper crustal molar ratios (Fe:Al 0.19) (Wedepohl,  
20 1995) or Amundsen Sea surface sediments (Fe:Al 0.26) (Angino, 1966). Interestingly, our  
21 observed pFe:pAl sedimentary ratios were similar to the ratio found in phytoplankton such as  
22 the BCR-414 certified reference material (freshwater phytoplankton) (Fe:Al = 1.01) used in  
23 this study (Table A1). Furthermore, the pFe:pAl ratio of sinking particles captured by the free  
24 floating PPS3 sediment traps (marine snow) had similar ratios of pFe:pAl of 1.02, 1.05, 0.91  
25 and 0.70 for stations E-1, E-3, E-5 and A3-2, respectively (Table 2). These observations  
26 highlight the major contribution of sinking biogenic material to the authigenic sediments in  
27 the area around the Kerguelen Plateau which was in contrast to the signature at station R-2  
28 due to its low productivity. The pFe in the sediments at all stations and primarily at station  
29 R-2 (as a fraction of its total weight) were similar to Weddell Sea surface sediments (Angino  
30 and Andrews, 1968) which ranged from 0.9 – 3.2%. In comparison, station R-2 has a mean  
31 value of 0.1 % Fe while station E-3, A3, F-L and E-4W had mean values of 0.3, 0.8, 1.5 and  
32 2.5% respectively. The low fraction of Fe within the authigenic sediment at R-2 indicates

1 limited pFe supply at this station in comparison to either the Weddell Sea or the Kerguelen  
2 Plateau presented here.

### 3 **3.4 Plateau, reference and polar front stations**

4 The reference station (R-2) has a bottom depth of 2528 m and is characterised by low surface  
5 Chl *a* concentrations (Lasbleiz et al., 2014) and nutrient concentrations characteristic of  
6 HNLC waters (Blain et al., 2014). Station F-L is approximately 313 km northeast of  
7 Kerguelen Island with a bottom depth of 2690 m and represents the northern PF. Station F-L  
8 is downstream of Kerguelen Island, with the PF delivering waters that originated near station  
9 R-2. In this case, the waters crossing Station F-L have interacted with both the plateau and  
10 shallow coastal waters of Kerguelen Island. In contrast, station A3 is located over the  
11 Kerguelen Plateau and has a bottom depth of 527 m, making it the shallowest station sampled  
12 for trace metal analysis of suspended particles and one of the most likely to be influenced by  
13 resuspension of shelf sediments (Fig. 1). The proximity of the station to Heard and Kerguelen  
14 Island (roughly half way between the two) means that fluvial and glacial runoff may also  
15 drive fertilisation at this site. However, the hydrography of the area dictates that waters which  
16 previously interacted with upstream Heard Island are a more likely source to A3 than  
17 downstream Kerguelen Island (Park et al., 2008).

18 The pFe, pAl and pMn concentrations at the reference station (R-2) only increase slightly  
19 towards the sea floor; however, enrichment in pFe, pAl and primarily pMn is evident at 500 m  
20 likely due to proximity to the Leclaire Rise (Fig. 3) (discussed in detail below). The northern  
21 PF station (F-L) exhibits moderate concentrations of pFe, pAl and pMn throughout the water  
22 column, somewhat higher than the reference station, and much higher concentrations are  
23 observed in close proximity to the sea floor. It should be noted that the deepest sample at R-2  
24 was 148 m above the seafloor, while at F-L it was only 90 m above the sea floor and this  
25 could well explain the observed difference, given the strong decrease of nepheloid layers  
26 away from the seabed (Blain et al., 2007; Jouandet et al., 2014).

27 Profiles of pFe and pAl in the 1 - 53  $\mu\text{m}$  size range from station R-2, A3 and F-L are shown in  
28 Figure 3. The plateau station (A3) was sampled twice during the study (A3-1 and A3-2),  
29 separated by 20 days. Surface chlorophyll images revealed that between visits to the site, a  
30 large bloom developed in the vicinity and extended over the site, and was beginning to fade  
31 again by the time of the second sampling (Trull et al., 2014). Thus, station A3-1 can be

1 thought of as pre-bloom and A3-2 as post-bloom conditions. Particulate Fe, Al and Mn  
2 generally increased towards the sea floor at station A3, with the exception of a slight  
3 enrichment below the mixed layer during the second visit (A3-2) to the station in the  $> 53 \mu\text{m}$   
4 size fraction (Fig. 4). To investigate the progression of pFe through time, we integrated the  
5 pFe throughout the full water column, and observed a decrease in the pFe stock from 9.1 to  
6  $4.5 \text{ mmol m}^{-2}$  between the first and second visit to station A3. This translates to a 51%  
7 reduction in pFe for all size classes combined (i.e.  $>1 \mu\text{m}$ ). However, if we look closer at the  
8 pFe distribution only within the surface mixed layer (165 m) between A3-1 and A3-2, we  
9 observe a loss of 70% of the integrated total pFe ( $>1\mu\text{m}$ ) (Fig. 4). Concurrently, using an  
10 Underwater Vision Profiler to track particle size distribution, Jouandet et al., (2014) noted a 4  
11 fold increase in particle numerical abundance through the full water column. Their one  
12 dimensional particle dynamic model supported the hypothesis that the increase in biogenic  
13 particles, due to blooming conditions, resulted in the rapid formation of large particles due to  
14 coagulation and subsequent vertical transport to the base of the mixed layer. This result is  
15 supported in the current data set, in that we see a large decrease in small pFe particles within  
16 the mixed layer and a moderate increase in large pFe particles at the base of the mixed layer  
17 when comparing pre (A3-1) to post (A3-2) bloom conditions (Fig. 4). Furthermore, we  
18 observed an increase in biogenic pFe within the surface mixed layer between A3-1 and A3-2  
19 (Section 3.7).

20 Thus, it appears that physical aggregation within the mixed layer of the particles onto  
21 biogenic phyto-aggregates during the bloom development and export to the base of the mixed  
22 layer, combined with significantly lower concentrations above the seafloor resulted in the  
23 observed 51% reduction in pFe ( $>1 \mu\text{m}$ ) between A3-1 and A3-2. The significantly lower  
24 concentration at 440m during the post-bloom conditions of A3-2 may be due to increased  
25 small particle scavenging resulting from sinking phyto-aggregates or alternatively, small-scale  
26 variation in the thickness of the nepheloid layer.

### 27 **3.5 Elemental ratios at stations R-2, F-L and A3**

28 As station A3 is located over the Kerguelen Plateau and also is in close proximity to fluvial  
29 and glacial runoff from Heard Island, we would expect the trace metal source signature of  
30 suspended particles to be unique here in comparison to our reference (R-2) and PF (F-L)  
31 stations. The particles over the Kerguelen Plateau were characterised by very high pFe (0.94 –  
32 30.4 nM) and pAl (1.5 – 58.6 nM) with concentrations an order of magnitude higher than R-2

1 (<DL-1.35 nM Fe and <DL – 2.08 nM Al). The reference station was characterised by low  
2 surface Chl *a* concentrations characteristic of HNLC waters (Lasbleiz et al., 2014), however,  
3 it is relatively close to the Leclaire Rise; a seamount with its shallowest point 135 km west  
4 northwest of station R-2 rising up to approximately 395 m. The Leclaire Rise extends to 70km  
5 northwest of station R-2 where it reaches a depth of approximately 550 m. It is important to  
6 recall in this context that the PF divides the northeast flowing AASW from the eastward  
7 flowing SASW to the north (Park et al., 2008). Classical theory suggests that this  
8 oceanographic feature should block much of the enrichment from the Leclaire Rise to station  
9 R-2. However, enrichment was evident in the vertical profiles of pFe, pMn and pAl at station  
10 R-2 at 500 m depth (Fig. 3).

11 Figure 5 illustrates the full water column elemental ratios at the reference station (R-2) in  
12 comparison to the Kerguelen Plateau stations (A3-1 and A3-2) and reveals that Mn:Fe as well  
13 as Ba:Al are strikingly unique. At station R-2, below 500 m, we see Mn:Fe 2x higher than A3,  
14 Mn:Al 4.5x higher and Ba:Al ratios 10x higher than at A3, making this source signature  
15 relatively clear (Table 2). The unique ratios below 500 m at R-2, may arise from a source of  
16 dissolved or particulate Mn (uncoupled from pFe and pAl) from the Leclaire Rise.  
17 Furthermore, the elemental ratios over station A3 are generally much lower (Fig. 5) due to  
18 high pFe and pAl supply over the Kerguelen Plateau that is relatively deficient in pMn such as  
19 would be found in glacial runoff that has a signature which reflects fresh weathering of  
20 basaltic rocks (Doucet et al., 2005). This source theory is supported by the observation of  
21 high dissolved Mn (dMn) near the Leclaire Rise (Qu  rou   et al., 2015) and uniquely high  
22 pMn:pFe in sediments found below station R-2 (Table 2). Surface water particulate trace  
23 metals also reveal distinct differences. The ratios of pFe:pAl, pMn:pAl and pMn:pFe all  
24 increase from the bottom of the mixed layer to the surface at stations R-2 and F-L (Fig. 5).  
25 This profile characteristic is in contrast to stations A3-1. The observed modification of the  
26 elemental ratios in the surface mixed layer at R-2 and F-L is most likely due to biological  
27 uptake of dissolved trace elements and conversion into the biogenic particulate fraction.

28 Particulate Al and pFe were closely coupled across all stations (Spearman's RHO  $R=0.91$   
29  $P<0.01$   $n=70$ ). However, pAl and pMn, although still strongly correlated ( $P=0.80$   $P<0.01$   
30  $n=70$ ), appeared more variable than pFe versus pAl. Figure 6 illustrates this variability in the  
31 pMn in comparison to pAl as a function of its location within the study area. The observed  
32 variability in pMn but not pFe relative to pAl highlights the uncoupling between some of the

1 sources of pMn and pFe. Specifically, the observed variability points to a uniquely high  
2 Mn:Fe source either in the authigenic sediments of the Leclaire Rise and/or a hydrothermal  
3 source (German et al., 1991), or a process whereby pAl is preferentially stripped out with  
4 distance from the source. A study by Shigemitsu et al. (2013) showed that the concentration  
5 of pAl in suspended particulate material in the Intermediate Water of the Sea of Okhotsk  
6 (western Pacific Ocean), decreased with distance from the shelf source preferentially in  
7 relation to pFe and pMn. They concluded that increasing pFe:pAl and pMn:pAl ratios  
8 occurred with distance from the source and suggested that the denser, lithogenic particles  
9 settled out preferentially, stripping out pAl. Furthermore, they found pFe became associated  
10 with organic matter more readily than pAl and therefore, remained suspended in the water  
11 column more readily than pAl. These processes could explain the observed modification of  
12 the elemental ratios between stations R-2, A3 and possibly F-L. The stations that were in  
13 close proximity to the shelf source such as A3-1 and A3-2 were indeed enriched in lithogenic  
14 pAl and as such pFe:pAl was relatively low (Fig. 5). In contrast, F-L was at the greatest  
15 distance from a sedimentary source and displayed the highest pFe:pAl ratio, whereas station  
16 R-2, being relatively close to the Leclaire rise, had an intermediate ratio.

17

### 18 **3.6 What are the sources of particulate trace metals over the plateau and** 19 **downstream?**

20 The high particulate trace metal concentrations found at 440 m, at A3-1 and A3-2, near the  
21 sea floor, most likely originated from resuspension of deep (~500 m) shelf sediments. The  
22 cause of the variability between A3-1 and A3-2 at this depth remains unclear, but could  
23 reflect small scale variability in the depth of the nepheloid layer or be the result of temporal  
24 variability due to the action of tides and internal waves (McCave, 1986). The pMn:pAl,  
25 pMn:pFe and pBa:pAl ratios for A3-1 and A3-2 are similar from the sea floor to the  
26 approximate base of the surface mixed layer, with values higher than the mean crustal ratios  
27 (Taylor and McLennan, 1985), but lower than either basalt (Doucet et al., 2005) or the  
28 underlying sediment ratios (Table 2). Within the surface mixed layer, A3-1 maintains similar  
29 ratios to the deep water column, while at A3-2 the ratios diverge towards the surface. The  
30 particulate trace metal signature within the mixed layer at A3-2 increases in pMn and pBa  
31 relative to pAl, which is most likely driven by biogenic conversion of dissolved bioessential  
32 elements into biogenic particles (section 3.7).

1 Glacial flour is the result of mechanical erosion of bed rock by glaciers. Typical particle sizes  
2 are within the silt size range but can overlap with clays (0.002 - 0.063 mm). Recent research  
3 suggests that Fe sourced from glacial erosion can be a major source of bioavailable Fe to the  
4 Southern Ocean (Poulton and Raiswell, 2005; Raiswell et al., 2008a, 2008b, 2006). Assuming  
5 no mixing and a dilute suspension, Stoke's law predicts that the small grain size of glacial  
6 flour allows it to remain suspended within a 500 m water column for between 2 and 2500  
7 days or within a 165m mixed layer for 1 to 831 days depending on particle size. Certainly,  
8 mixing within the surface mixed layer would increase this duration significantly, meaning that  
9 glacial and fluvial input from both Heard and Kerguelen Island could remain suspended in the  
10 mixed layer for long enough to travel well past any of the stations in the present study,  
11 excluding the reference station (R-2). Furthermore, it has been shown that 2 – 3 % of the Fe  
12 within glacial rock flour can be leached into the dissolved size fraction ( $< 0.2 \mu\text{m}$ ) with  
13 ultrapure water; a large proportion of which should be bioavailable (Schroth et al., 2009). It is  
14 thought that this dFe is leached from nanoparticulate Fe (oxyhydr)oxides in glacial rock flour  
15 over time (Raiswell, 2011; Raiswell et al., 2010) following an exponential decay, so it is  
16 possible that this source could be excluded from the  $< 0.2 \mu\text{m}$  dissolved fraction, but included  
17 in the 1-53  $\mu\text{m}$  particulate fraction presented here. This is especially true of nanoparticulate  
18 Fe that is attached to the surface of larger sediment grains as has been observed previously in  
19 glacial sediments (Shaw et al., 2011). Given that the particulate fraction is generally an order  
20 of magnitude higher in concentration than the dissolved fraction, this source may well be  
21 more significant in stimulating phytoplankton blooms than previously estimated. Overall,  
22 station A3 appeared to be directly fertilised by resuspension of shelf sediments at depth, and  
23 entrainment of this pFe-rich water occurred during events that deepen the mixed layer  
24 periodically. However, lateral supply above the mixed layer of small particles from shallow  
25 coastal sources around Heard Island, including glacial melt waters, cannot be ruled out.

### 26 **3.7 Biogenic and sedimentary particulate trace metals**

27 If we assume that all particulate phosphorus (pP) is of biogenic origin, we can calculate the  
28 biogenic Fe fraction of the total Fe concentration by normalising to pP and comparing with  
29 published elemental ratios of Southern Ocean diatoms (Planquette et al., 2013). For the  
30 calculations we used the upper limit of Fe:P ( $1.93 \text{ mmol mol}^{-1}$ ) reported by Twinning et al.  
31 (2004) for Southern Ocean diatom assemblages. Given that pP and POC are remineralised  
32 throughout the water column and are generated within the surface mixed layer, calculations of

1 biogenic trace metals will only be valid within the surface mixed layer, as the concentration of  
2 pP and POC decreases strongly with depth. It should also be noted that Kerguelen Island  
3 basalts and upper continental crust can contribute particulate phosphorus concomitantly with  
4 pFe to the particulate pool. However the Fe:P ratio found within Kerguelen Island basalts and  
5 the continental crust is 12.8 and 25.8 (mol:mol) respectively (Gautier et al., 1990; Wedepohl,  
6 1995). Thus, the factor of 1000 increase in pP observed within suspended particles compared  
7 to these rock sources indicates that this pP is likely produced *insitu* within the mixed layer  
8 from dissolved  $\text{PO}_4^-$  rather than supplied from rock weathering together with Fe.  
9 Furthermore, within the upper 200 m of the water column, biogenic Fe correlates significantly  
10 with both fluorescence (Spearmans RHO  $R = 0.518$ ,  $P < 0.05$ ,  $n = 30$ ) and dissolved oxygen  
11 (Spearmans RHO  $R = 0.507$ ,  $P < 0.05$ ,  $n = 30$ ) confirming the autotrophic composition of the  
12 particles identified as high in biogenic Fe. Figure 3 illustrates the contribution of biogenic Fe  
13 in surface waters at stations R-2, A3 and F-L. Station R-2 and F-L have biogenic Fe fractions  
14 that are higher near the surface than at depth (Fig. 3). In contrast, at stations A3-1 and A3-2,  
15 biogenic Fe and Mn only make up a relatively small fraction of the total pFe throughout the  
16 water column although at station A3-2 we see a slight increase in biogenic pFe towards the  
17 surface, corresponding with the development of a bloom. Biogenic Fe at stations A3-1 and  
18 A3-2 constitutes less than 1 and 5% respectively of the total Fe. The low biogenic fraction at  
19 station A3-1 most likely results from an excess of lithogenic Fe, Al and Mn to the water  
20 column from the shelf sediments as well as fluvial/glacial runoff from nearby Islands of the  
21 Kerguelen Archipelago, which are excess to demand. A similar pattern was observed during  
22 a study located in the Amundsen Sea (Planquette et al., 2013) where the percentage of  
23 biogenic Fe (full water column mean) reduced with proximity to the trace metal source.

24

25 Alternatively, the relative importance of sedimentary input at each of the stations can be  
26 gauged by observing the pMn:pAl molar ratio within suspended particles and comparing these  
27 to known molar ratios of pMn:pAl within Kerguelen Island basalts, A3 authigenic sediments  
28 and R-2 authigenic sediments (Fig. 6). At station A3 we see that almost all the suspended  
29 particles lie within the ratio of plateau sediments and Kerguelen Island basalts with the  
30 remaining suspended particles associated with the development of a bloom in surface waters  
31 at A3-2, which is also where we see an increase in biogenic Fe. Mid-depth suspended  
32 particles at E4-W (red dots) also lie between Kerguelen Island basalts and plateau sediments,



1 indicating a similar source to station A3. The reference station exhibits highly modified  
2 pMn:pAl molar ratios within the suspended particles and its underlying sediment. This  
3 modification is most likely due to biogenic incorporation of bioessential elements such as Mn  
4 into particles. The remaining stations are intermediate between A-3 and R-2.

5

### 6 **3.8 Pseudo-Lagrangian, recirculation-structure**

7 Station E-4W has trace metal concentrations, elemental ratios and community size structure  
8 (Trull et al., 2014) similar to A3 and as such, will be excluded from the discussion in this  
9 section. The remaining recirculation structure stations exhibit profiles of pFe and pMn which  
10 show a minimum at approximately 150 - 175 m (Fig. 7). Our detailed depth profile indicates  
11 that the pFe and pMn minima coincide with the remnant winter water temperature minimum  
12 (Fig. 8). Interestingly, Blain et al. (2014) also estimated a winter water depth of  
13 approximately 150 m. They observed at 150m, that nitrate and phosphate profiles within the  
14 recirculation feature, from multiple years and seasons, converged with striking consistency.  
15 Particulate Fe and pMn, concentrations increase above and below the temperature minimum,  
16 however, pAl only increases below 175 m. Particulate Al is stripped out preferentially with  
17 settling lithogenics while pFe and pMn are retained either through conversion to the biogenic  
18 particulate fraction (uptake) or adsorbed onto organic particles. It should be noted here that  
19 the work of Raiswell (2011) indicates that iceberg and glacially derived Fe nanoparticulate  
20 material is typically high in Fe and low in Al. Thus, supply of glacially derived  
21 nanoparticulate Fe from Kerguelen Island, via the north east of the recirculation structure  
22 could also cause the observed high Fe, low Al surface enrichment within the recirculation  
23 structure.

24 Given that the pFe and pMn minima coincides with the remnant-winter-water temperature  
25 minimum, the total amount of particulate trace metals distributed throughout the winter mixed  
26 layer must be lower than during summer. This is counterintuitive if sediment resuspension is  
27 the primary source of particulate trace metals into the recirculation feature. During winter we  
28 would expect increased wind mixing, leading to more entrainment of pFe over the plateau and  
29 more supply into the recirculation feature leading to a maximum at the temperature minimum.  
30 Given that we observe the inverse situation, supply into the recirculation structure must be

1 low during winter. Thus, we suggest that the lateral supply of fluvial and glacial derived  
2 particulate trace metals must be an important source. This source would be expected to reduce  
3 in winter when precipitation as snow and glacial freezing is at a maximum and conversely,  
4 during spring, snow and ice melt and rainfall increases runoff into the coastal areas and  
5 induces a fertilisation event downstream of Heard and Kerguelen Islands. Kerguelen Island is  
6 a subantarctic island, and its climatology is cold and wet, with the Port-aux-Francais weather  
7 station recording mean daily temperatures of 2.1° C in winter and 8.2° C in summer and year  
8 round consistent precipitation (730 mm annually) (Meteo France). It should be noted that due  
9 to its sheltered location and sea level altitude, the Port-aux-Francais location is relatively mild  
10 compared to the west coast and interior of the island which is estimated to receive 3 times the  
11 rainfall of the east coast, or 2124 mm annually. Therefore, having a climate of high  
12 precipitation and seasonal thawing, increased seasonal runoff can be expected in spring and  
13 summer from Kerguelen Island.

14 The importance of glacial/fluvial sources in supplying dissolved Fe and Mn into coastal  
15 waters to the north east of Kerguelen, north of the PF, has been shown previously by  
16 Bucciarelli et al., (2001). The authors found a linear relationship between dissolved Fe and  
17 lithogenic silica and suggested that this was indicative of weathering of silicate rich minerals  
18 that characterise the Kerguelen Islands with a concomitant release of dissolved Fe and Mn.  
19 Indeed in the present study, using the lithogenic and biogenic silica data presented in Closset  
20 et al., (2014), total particulate Fe correlated significantly with total lithogenic silica ( $R=0.76$ ,  
21  $P<0.01$ ) but not with biogenic silica. However, this significant correlation was not limited to  
22 the coastal regions in the present study and instead was observed for all stations and depths  
23 combined. Bucciarelli et al., (2001) found an exponential decrease in dissolved Fe with  
24 distance from the coast, further supporting their theory of a dominant coastal source in this  
25 region. This exponential decrease would be expected to apply to the particulate fraction also;  
26 however, it appears that even with an exponential decrease in pFe with distance from the  
27 coast, particulate Fe enrichment, sourced from fluvial runoff, is evident on the southern side  
28 of the PF within the recirculation feature.

29 The hypothesis of pFe supply from north of the PF into the eastern side of the recirculation  
30 feature via the mixing zone is supported by radium isotope data (Sanial et al., 2014) collected  
31 during the KEOPS2 mission. Apparent radium ages derived from the ratio of  $^{224}\text{Ra}/^{223}\text{Ra}$   
32 (and using the ratio observed within the Baie des Baleiniers as the starting time) suggest that

1 the age of water since fertilisation within the recirculation feature was only 5-8 days. This  
2 indicates that there is likely rapid transfer across the PF of fertilised waters which were  
3 sourced from nearby shallow coastal areas such as the Baie des Baleiniers, Kerguelen Island.  
4 The authors go on to highlight that the heterogeneous distribution of  $^{224}\text{Ra}$  and  $^{223}\text{Ra}$  indicates  
5 that transfer across the polar front is sporadic in nature.

6 The observation of pFe enrichment in surface waters of the recirculation structure without  
7 proportional concentrations of pAl may be due to biological uptake and conversion from a  
8 bioavailable pool into the biogenic particulate pool. Settling of refractory lithogenics that are  
9 high in Al may also partially explain the observation. Alternatively or in combination, a high  
10 pFe, low pAl source such as nanoparticulate Fe characteristic of glacial/fluvial runoff  
11 (Hawkings et al., 2014; Raiswell et al., 2008b, 2006) on Kerguelen Island could explain this  
12 observation. Indeed, temperature and salinity profiles within the recirculation structure reveal  
13 fresher and warmer water within the upper 110 m than either R-2 or A3 stations suggesting  
14 that glacial/fluvial runoff from Kerguelen Island may well be delivering this high pFe, low  
15 pAl surface enrichment.

16

#### 17 **4 Conclusions**

18 This study has identified two distinct areas of Fe fertilisation in the vicinity of Kerguelen  
19 Island. Firstly, the plateau itself is a major source of resuspended shelf sediments to station  
20 A3 especially below the mixed layer. Secondly, fluvial and glacial runoff into coastal waters  
21 in combination with resuspension of shallow coastal sediments fertilises areas to the north of  
22 the PF, east of Kerguelen Island, but also across the PF and into the recirculation feature from  
23 the north-east. Indications of particle transport across the PF were observed at station R-2  
24 sourced from the Leclaire Rise to the north of the PF. Satellite imagery also revealed  
25 filaments clearly diverging from the main jet of the PF and into the north east of the  
26 recirculation structure. Within the recirculation structure, the correspondence of the winter  
27 water temperature minimum with the particulate trace metal minimum implies that a seasonal  
28 cycle is involved in the supply of trace elements. This is most likely driven by increased  
29 fluvial and glacial runoff in summer, associated with rainfall and basal melt and reduced  
30 supply in winter when snowfall and freezing conditions predominate. In this complex region,

1 it appears that weathering of the islands themselves are direct sources of new Fe and help  
2 stimulate the seasonal bloom that is significant in terms of the regional carbon cycle.

3 Over the mesoscale, it appears that physical processes associated with settling of refractory  
4 lithogenic particles was an important process in modifying the particulate elemental ratios.  
5 However, on the individual profile scale, biological processes seem important in modifying  
6 the elemental ratios in surface waters through preferential uptake of bio-essential elements,  
7 even from the particulate fraction.

8 Repeat sampling over the plateau provided a perspective on the persistence of the particulate  
9 Fe availability. Small particles containing pFe were efficiently transported out of the mixed  
10 layer during a bloom event over stations A3. This resulted in a 70% reduction in the  
11 integrated pFe stock within the mixed layer as a result of physical aggregation of small  
12 particles onto phyto-aggregates, presumably decreasing particle buoyancy and increasing  
13 export out of the mixed layer. This is likely to be an important aspect of the complex  
14 interaction between iron supply and biological availability, capable of mediating bloom  
15 duration and thus the efficiency of carbon sequestration.

16

## 17 **Appendix: Certified reference material analysis**

18 **Table A1:** Percentage recoveries of BCR-414 certified reference material. Certified and  
19 single lab values taken from the final report of the Commission of the European  
20 Communities, Community Bureau of Reference for BCR-414, EUR14558.

mg/kg	Rep 1	Rep 2	Rep 3	Mean	SD	RSD (%)	Certified	% recovery	single lab analysis	% recovery
Ba	34	26	32	31	4.0	13.1			31	99
Al	2243	1349	1943	1845	454.6	24.6			1800	102
Mn	278	284	283	282	3.4	1.2	299	94		
Fe	1874	1850	1878	1867	15.0	0.8	1850	101		

21

## 22 **Acknowledgements**

23 This work was supported by the Antarctic Climate and Ecosystems Cooperative Research  
24 Centre, University of Tasmania, Australia. This work was also supported by the French  
25 Research program of INSU-CNRS LEFE-CYBER (Les enveloppes fluides et

1 l'environnement –Cycles biogéochimiques, environnement et ressources), the French ANR  
2 (Agence Nationale de la Recherche, SIMI-6 program, ANR-10-BLAN-0614), the French  
3 CNES (Centre National d'Etudes Spatiales) and the French Polar Institute IPEV (Institut  
4 Polaire Paul–Emile Victor). We would like to thank the captain and the crew of the R.V.  
5 *Marion Dufresne*, Prof. Stephane Blain and Prof. Bernard Quéguiner as chief scientist and  
6 project coordinator of the KEOPS2 cruises, respectively. Leanne Armand was supported by  
7 grant Australian Antarctic Division, AAS grant #3214. Access to Sector Field ICP-MS  
8 instrumentation was supported through ARC LIEF funding (LE0989539).

9

## 1 References

- 2 Angino, E., 1966. Geochemistry of Antarctic pelagic sediments. *Geochim. Cosmochim. Acta*  
3 30, 939–961.
- 4 Angino, E., Andrews, R., 1968. Trace element chemistry, heavy minerals, and sediment  
5 statistics of Weddell Sea sediments. *J. Sediment. Res.* 38, 634–642.
- 6 Armand, L.K., Crosta, X., Quéguiner, B., Mosseri, J., Garcia, N., 2008. Diatoms preserved in  
7 surface sediments of the northeastern Kerguelen Plateau. *Deep Sea Res. Part II Top.*  
8 *Stud. Oceanogr.* 55, 677–692.
- 9 Barnola, J.M., Raynaud, D., Korotkevich, Y.S., Lorius, C., 1987. Vostok ice core provides  
10 160, 000-year record of atmospheric CO<sub>2</sub>. *Nat.* 329, 408–414.
- 11 Blain, S., Capparos, J., Guéneuguès, a., Obernosterer, I., Oriol, L., 2014. Distributions and  
12 stoichiometry of dissolved nitrogen and phosphorus in the iron fertilized region near  
13 Kerguelen (Southern Ocean). *Biogeosciences Discuss.* 11, 9949–9977.
- 14 Blain, S., Queguiner, B., Armand, L., Belviso, S., Bombled, B., Bopp, L., Bowie, A.R.,  
15 Brunet, C., Brussaard, C., Carlotti, F., Christaki, U., Corbiere, A., Durand, I., Ebersbach,  
16 F., Fuda, J.L., Garcia, N., Gerringa, L., Griffiths, B., Guigue, C., Guillerm, C., Jacquet,  
17 S.H.M., Jeandel, C., Laan, P., Lefevre, D., Lo Monaco, C., Malits, A., Mosseri, J.,  
18 Obernosterer, I., Park, Y.H., Picheral, M., Pondaven, P., Remenyi, T., Sandroni, V.,  
19 Sarthou, G., Savoye, N., Scouarnec, L., Souhaut, M., Thuiller, D., Timmermans, K.,  
20 Trull, T., Uitz, J., Van Beek, P., Veldhuis, M., Vincent, D., Viollier, E., Vong, L.,  
21 Wagener, T., 2007. Effect of natural iron fertilization on carbon sequestration in the  
22 Southern Ocean. *Nature* 446, 1070–1074.
- 23 Bopp, L., Kohfeld, K.E., Le Quéré, C., Aumont, O., 2003. Dust impact on marine biota and  
24 atmospheric CO<sub>2</sub> during glacial periods. *Paleoceanography* 18, 1–24.
- 25 Bowie, A.R., Townsend, A.T., Lannuzel, D., Remenyi, T.A., van der Merwe, P., 2010.  
26 Modern sampling and analytical methods for the determination of trace elements in  
27 marine particulate material using magnetic sector inductively coupled plasma-mass  
28 spectrometry. *Anal. Chim. Acta* 676, 15–27.
- 29 Bowie, A.R., van der Merwe, P., Trull, T., Quéroué, F., Fourquez, M., Planchon, F., Sarthou,  
30 G., Blain, S., 2014. Iron budgets for three distinct biogeochemical sites around the  
31 Kerguelen plateau (Southern Ocean) during the natural fertilization experiment KEOPS-  
32 2. *Biogeosciences Discuss.*
- 33 Boyd, P.W., Jickells, T., Law, C.S., Blain, S., Boyle, E.A., Buesseler, K.O., Coale, K.H.,  
34 Cullen, J.J., de Baar, H.J.W., Follows, M., Harvey, M., Lancelot, C., Levasseur, M.,  
35 Owens, N.P.J., Pollard, R., Rivkin, R.B., Sarmiento, J., Schoemann, V., Smetacek, V.,  
36 Takeda, S., Tsuda, A., Turner, S., Watson, A.J., Baar, H.J.W. De, 2007. Mesoscale iron  
37 enrichment experiments 1993-2005: Synthesis and future directions. *Science* (80- ). 315,  
38 612–617.

- 1 Bucciarelli, E., Bowie, A.R., Tréguer, P., 2001. Iron and manganese in the wake of the  
2 Kerguelen Islands (Southern Ocean). *Mar. Chem.* 73, 21–36.
- 3 Chever, F., Sarthou, G., Bucciarelli, E., Bowie, A.R., 2009. An iron budget during the natural  
4 iron fertilisation experiment KEOPS (Kerguelen Islands, Southern Ocean).  
5 *Biogeosciences* 7, 455–468.
- 6 Closset, I., Lasbleiz, M., Leblanc, K., Quéguiner, B., Cavagna, a.-J., Elskens, M., Navez, J.,  
7 Cardinal, D., 2014. Seasonal evolution of net and regenerated silica production around a  
8 natural Fe-fertilized area in the Southern Ocean estimated from Si isotopic approaches.  
9 *Biogeosciences Discuss.* 11, 6329–6381.
- 10 Cullen, J.T., Sherrell, R.M., 1999. Techniques for determination of trace metals in small  
11 samples of size-fractionated particulate matter: Phytoplankton metals off central  
12 California. *Mar. Chem.* 67, 233–247.
- 13 Cutter, G., Andersson, P., Codispoti, L., Croot, P., Francois, R., Lohan, M., Obata, H.,  
14 Rutgers van der Loeff, M., 2010. Sampling and Sample-handling Protocols for  
15 GEOTRACES Cruises.
- 16 De Baar, H.J.W., 2005. Synthesis of iron fertilization experiments: From the Iron Age in the  
17 Age of Enlightenment. *J. Geophys. Res.* 110, C09S16.
- 18 De Baar, H.J.W., de Jong, J.T., 2001. Distribution, sources and sinks of iron in seawater., in:  
19 Turner, D.R., Hunter, K.A. (Eds.), *The Biogeochemistry of Iron in Seawater*. IUPAC  
20 Series on Analytical and Physical Chemistry of Environmental Systems, pp. 123–253.
- 21 Doucet, S., Scoates, J.S., Weis, D., Giret, A., 2005. Constraining the components of the  
22 Kerguelen mantle plume: A Hf-Pb-Sr-Nd isotopic study of picrites and high-MgO  
23 basalts from the Kerguelen Archipelago. *Geochemistry, Geophys. Geosystems* 6, n/a–  
24 n/a.
- 25 Frew, R.D., Hutchins, D.A., Nodder, S., Sanudo-Wilhelmy, S., Tovar-Sanchez, A., Leblanc,  
26 K., Hare, C.E., Boyd, P.W., 2006. Particulate iron dynamics during FeCycle in  
27 subantarctic waters southeast of New Zealand. *Global Biogeochem. Cycles* 20.
- 28 Gautier, I., Weis, D., Mennessier, J.-P., Vidal, P., Giret, A., Loubet, M., 1990. Petrology and  
29 geochemistry of the Kerguelen Archipelago basalts ( South Indian Ocean )" evolution of  
30 the mantle sources from ridge to intraplate position. *Earth Planet. Sci. Lett.* 100, 59–76.
- 31 German, C., Campbell, A., Edmond, J., 1991. Hydrothermal scavenging at the Mid-Atlantic  
32 Ridge: modification of trace element dissolved fluxes. *Earth Planet. Sci. Lett.* 107, 101–  
33 114.
- 34 Hawkings, J.R., Wadham, J.L., Tranter, M., Raiswell, R., Benning, L.G., Statham, P.J.,  
35 Tedstone, A., Nienow, P., Lee, K., Telling, J., 2014. Ice sheets as a significant source of  
36 highly reactive nanoparticulate iron to the oceans. *Nat. Commun.* 5, 3929.

- 1 Johnson, K.S., Gordon, R.M., Coale, K.H., 1997. What controls dissolved iron concentrations  
2 in the world ocean? *Mar. Chem.* 57, 137–161.
- 3 Jouandet, M.-P., Jackson, G. a., Carlotti, F., Picheral, M., Stemmann, L., Bowie, A.R., 2014.  
4 Rapid formation of large aggregates during the spring bloom of Kerguelen Island:  
5 observations and model comparisons. *Biogeosciences Discuss.* 11, 4949–4993.
- 6 Lasbleiz, M., Leblanc, K., Bowie, A.R., Ras, J., Cornet-Barthaux, V., Hélias Nunige, S.,  
7 Quéguiner, B., 2014. Pigments, elemental composition (C, N, P, Si) and stoichiometry of  
8 particulate matter, in the naturally iron fertilized region of Kerguelen in the Southern  
9 Ocean. *Biogeosciences Discuss.* 11, 8259–8324.
- 10 Laurenceau, E.C., Trull, T., Davies, D.M., Bray, S.G., Doran, J., Planchon, F., Cavagna, A.-J.,  
11 Waite, A., 2014. The relative importance of phytodetrital aggregates and fecal matter in  
12 the control of export fluxes from naturally iron-fertilised waters near the Kerguelen  
13 plateau. *Biogeosciences Discuss.* 13623–13673.
- 14 Martin, J.H., 1990. Glacial-interglacial CO<sub>2</sub> change: The iron hypothesis. *Paleoceanography*  
15 5, 1–13.
- 16 McCave, I.N., 1986. Local and global aspects of the bottom nepheloid layers in the world  
17 ocean. *Netherlands J. Sea Res.* 20, 167–181.
- 18 Moffett, J.W., 2001. Transformations Among Different Forms of Iron in the Ocean, in:  
19 Turner, D.R., Hunter, K. a. (Eds.), *The Biogeochemistry of Iron in Seawater*. John Wiley  
20 & Sons, pp. 343–372.
- 21 Park, Y.-H., Roquet, F., Durand, I., Fuda, J.-L., 2008. Large-scale circulation over and around  
22 the Northern Kerguelen Plateau. *Deep Sea Res. Part II Top. Stud. Oceanogr.* 55, 566–  
23 581.
- 24 Planchon, F., Ballas, D., Cavagna, A.-J., Bowie, A.R., Davies, D.M., Trull, T., Laurenceau,  
25 E.C., van der Merwe, P., Dehairs, F., 2014. Carbon export in the naturally iron-fertilized  
26 Kerguelen area of the Southern Ocean based on the 234 Th approach. *Biogeosciences*  
27 *Discuss.* 15991–16032.
- 28 Planquette, H., Sherrell, R.M., Stammerjohn, S., Field, M.P., 2013. Particulate iron delivery  
29 to the water column of the Amundsen Sea, Antarctica. *Mar. Chem.* 153, 15–30.
- 30 Pollard, R., Salter, I., Sanders, R., Lucas, M., 2009. Southern Ocean deep-water carbon export  
31 enhanced by natural iron fertilization. *Nature* 457, 577–581.
- 32 Poulton, S.W., Raiswell, R., 2005. Chemical and physical characteristics of iron oxides in  
33 riverine and glacial meltwater sediments. *Chem. Geol.* 218, 203–221.
- 34 Quéguiner, B., 2013. Iron fertilization and the structure of planktonic communities in high  
35 nutrient regions of the Southern Ocean. *Deep Sea Res. Part II Top. Stud. Oceanogr.* 90,  
36 43–54.



- 1 Qu  rou  , F., Sarthou, G., Planquette, H., Bucciarelli, E., Chever, F., van der Merwe, P.,  
2 Lannuzel, D., Townsend, A.T., Cheize, M., Blain, S., D'Ovidio, F., Bowie, A.R., 2015.  
3 High variability of dissolved iron concentrations in the vicinity of Kerguelen Island  
4 (Southern Ocean). *Biogeosciences Discuss.* 231–270.
- 5 Raiswell, R., 2011. Iceberg-hosted nanoparticulate Fe in the Southern Ocean: Mineralogy,  
6 origin, dissolution kinetics and source of bioavailable Fe. *Deep Sea Res. Part II Top.*  
7 *Stud. Oceanogr.* 58, 1364–1375.
- 8 Raiswell, R., Benning, L.G., Tranter, M., Tulaczyk, S., 2008a. Bioavailable iron in the  
9 Southern Ocean: The significance of the iceberg conveyor belt. *Geochem. Trans.* 9,  
10 article no. 7.
- 11 Raiswell, R., Benning, L.G.L., Davidson, L., Tranter, M., 2008b. Nanoparticulate  
12 bioavailable iron minerals in icebergs and glaciers. *Mineral. Mag.* 72, 345–348.
- 13 Raiswell, R., Tranter, M., Benning, L.G., Siegert, M., De'ath, R., Huybrechts, P., Payne, T.,  
14 De'ath, R., 2006. Contributions from glacially derived sediment to the global iron  
15 (oxyhydr)oxide cycle: Implications for iron delivery to the oceans. *Geochim.*  
16 *Cosmochim. Acta* 70, 2765–2780.
- 17 Raiswell, R., Vu, H.P., Brinza, L., Benning, L.G., 2010. The determination of labile Fe in  
18 ferrihydrite by ascorbic acid extraction: Methodology, dissolution kinetics and loss of  
19 solubility with age and de-watering. *Chem. Geol.* 278, 70–79.
- 20 Sanial, V., van Beek, P., Lansard, B., Souhaut, M., Kestenare, E., D'Ovidio, F., Blain, S.,  
21 2014. Use of Ra isotopes to deduce rapid transfer of sediment-derived inputs off  
22 Kerguelen. *Biogeosciences Discuss.* 14023–14061.
- 23 Savoye, N., Trull, T., Jacquet, S.H.M., Navez, J., Dehairs, F., 2008. 234Th-based export  
24 fluxes during a natural iron fertilization experiment in the Southern Ocean (KEOPS).  
25 *Deep Sea Res. Part II Top. Stud. Oceanogr.* 55, 841–855.
- 26 Schroth, A.W., Crusius, J., Sholkovitz, E.R., Bostick, B.C., 2009. Iron solubility driven by  
27 speciation in dust sources to the ocean. *Nat. Geosci.* 2, 337–340.
- 28 Shaw, T.J., Raiswell, R., Hexel, C.R., Vu, H.P., Moore, W.S., Dudgeon, R., Smith, K.L.,  
29 2011. Input, composition, and potential impact of terrigenous material from free-drifting  
30 icebergs in the Weddell Sea. *Deep Sea Res. Part II Top. Stud. Oceanogr.* 58, 1376–1383.
- 31 Shigemitsu, M., Nishioka, J., Watanabe, Y.W., Yamanaka, Y., Nakatsuka, T., Volkov, Y.N.,  
32 2013. Fe/Al ratios of suspended particulate matter from intermediate water in the  
33 Okhotsk Sea: Implications for long-distance lateral transport of particulate Fe. *Mar.*  
34 *Chem.* 157, 41–48.
- 35 Sunda, W.G., 2001. Bioavailability and Bioaccumulation of Iron in the Sea, in: Turner, D.R.,  
36 hunter, K.H. (Eds.), *The Biogeochemistry of Iron in Seawater. IUPAC Series on*  
37 *Analytical and Physical Chemistry of Environmental Systems*, pp. 41–84.

- 1 Taylor, S.R., McLennan, S.M. (Scott M., 1985. The continental crust, its composition and  
2 evolution : an examination of the geochemical record preserved in sedimentary rocks /  
3 Stuart Ross Taylor, Scott M. McLennan. Oxford ; Melbourne : Blackwell Scientific  
4 Publications.
- 5 Townsend, A.T., 2000. The accurate determination of the first row transition metals in water,  
6 urine, plant, tissue and rock samples by sector field ICP-MS. *J. Anal. At. Spectrom.* 15,  
7 307–314.
- 8 Trull, T., Davies, D.M., Dehairs, F., Cavagna, A.-J., Lasbleiz, M., Laurenceau, E.C.,  
9 D'Ovidio, F., Planchon, F., Queguiner, B., Blain, S., 2014. Chemometric perspectives on  
10 plankton community responses to natural iron fertilization over and downstream of the  
11 Kerguelen plateau in the Southern Ocean. *Biogeosciences Discuss.* 13841–13903.
- 12 Twining, B.S., Baines, S.B., Fisher, N.S., 2004. Element stoichiometries of individual  
13 plankton cells collected during the Southern Ocean Iron Experiment (SOFEX). *Limnol.*  
14 *Oceanogr.* 49, 2115–2128.
- 15 Van Beek, P., Bourquin, M., Reyss, J.L., Souhaut, M., Charette, M.A., Jeandel, C., 2008.  
16 Radium isotopes to investigate the water mass pathways on the Kerguelen Plateau  
17 (Southern Ocean). *Deep Sea Res. Part II Top. Stud. Oceanogr.* 55, 622–637.
- 18 Watson, A.J., Bakker, D.C.E., Ridgwell, A.J., Boyd, P.W., Law, C.S., 2000. Effect of iron  
19 supply on Southern Ocean CO<sub>2</sub> uptake and implications for 407.
- 20 Wedepohl, K.H., 1995. The composition of the continental crust. *Geochim. Cosmochim. Acta*  
21 59, 1217–1232.
- 22 Zhang, Y., Lacan, F., Jeandel, C., 2008. Dissolved rare earth elements tracing lithogenic  
23 inputs over the Kerguelen Plateau (Southern Ocean). *Deep Sea Res. Part II Top. Stud.*  
24 *Oceanogr.* 55, 638–652.
- 25

1 Table 1. KEOPS2 sampling locations and station types.

2

	<b>A3-1</b>	<b>A3-2</b>	<b>R-2</b>	<b>F-L</b>	<b>E-1</b>	<b>E-3</b>	<b>E-5</b>	<b>E-4E</b>	<b>E-4W</b>
<b>Station type</b>	Kerguelen Plateau 1st visit	Kerguelen Plateau 2nd visit	HNLC reference station	Northern Polar Front	recirculation structure	recirculation structure	recirculation structure	Eastern recirculation structure	Western recirculation structure
<b>Sampling date</b>	20/10/2011	16/11/2011	25/10/2011	6/11/2011	29/10/2011	3/11/2011	18/11/2011	13/11/2011	11/11/2011
<b>Latitude (S)</b>	50° 37.7574'	50° 37.4306'	50° 21.52'	48° 31.394'	48° 29.5728'	48° 42.1334'	48° 24.698'	48° 42.9218'	48° 45.927'
<b>Longitude (E)</b>	72° 4.8193'	72° 3.3366'	66° 43.00'	74° 40.036'	72° 14.1467'	71° 58.0027'	71° 53.7894'	72° 33.7792'	71° 25.51'
<b>Bottom depth (m)</b>	505	505	2528	2690	2050	1910	1920	2200	1400
<b>Time series</b>	Yes	Yes	No	No	Yes	Yes	Yes	No	No
<b>Particulate</b>									
<b>Trace Metals</b>	Yes	Yes	Yes	Yes	Yes	Yes	Yes	Yes	Yes
<b>POC PON</b>	Yes	Yes	Yes	Yes	Yes	Yes	Yes	Yes	Yes
<b>Sediment samples</b>	Yes	Yes	Yes	Yes	No	Yes	No	Yes	Yes
<b>Sediment trap samples</b>	No	Yes	No	No	Yes	Yes	Yes	No	No

3

1

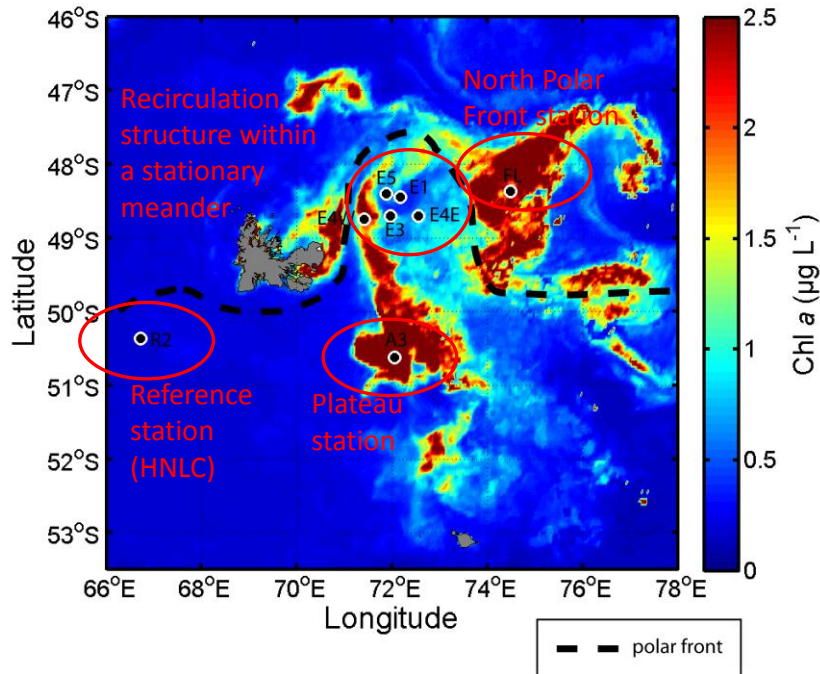
2 Table 2. Mean elemental molar ratios of marine snow particles captured in free-floating  
 3 sediment traps, particulate matter (<53  $\mu\text{m}$ ) below the mixed layer and authigenic  
 4 sediments at each station. Note that station TEW-1 is a near-coastal station located  
 5 within Hillsborough Bay, Kerguelen Island. Station TEW-1 is not discussed in detail in  
 6 the MS as no samples were collected for suspended particles; however, details are  
 7 included here to show the influence of close proximity to the island and fluvial/glacial  
 8 sources.

<b>Sediment trap @ 210 m</b>				
<b>m</b>	<b>pFe:pAl</b>	<b>pMn:pAl</b>	<b>pMn:pFe</b>	<b>pBa:pAl</b>
<b>A3-2</b>	0.70	0.008	0.011	0.025
<b>E-1</b>	1.02	0.009	0.009	0.162
<b>E-3</b>	1.05	0.010	0.010	0.285
<b>E-5</b>	0.91	0.008	0.009	0.318
<b>Suspended particles mean (&gt; MLD)</b>				
<b>A3-1</b>	0.53	0.007	0.013	0.027
<b>A3-2</b>	0.63	0.009	0.014	0.034
<b>R-2</b>	0.65	0.036	0.059	0.322
<b>F-L</b>	0.77	0.020	0.027	0.190
<b>E-4E</b>	0.86	0.037	0.045	0.383
<b>E-4W</b>	0.63	0.014	0.021	0.078
<b>E-1</b>	0.68	0.023	0.034	0.185
<b>E-3</b>	0.71	0.024	0.033	0.258
<b>E-5</b>	0.68	0.020	0.030	0.260
<b>Sediment analysis</b>				
<b>TEW-1</b>	1.10	0.013	0.012	0.003
<b>A3-1</b>	0.87	0.011	0.013	0.026
<b>R-2</b>	0.73	0.063	0.086	0.892
<b>F-L</b>	0.82	0.016	0.019	0.040
<b>E-4W</b>	0.81	0.013	0.016	0.013
<b>E-3</b>	0.93	0.015	0.016	0.125
<b>Kerguelen Archipelago</b>				
<b>Basalt mean (Gautier et al., 1990)</b>	0.08 - 0.49	0.004 - 0.010	0.021 - 0.050	0.002- 0.004
<b>Upper continental crust (Wedepohl, 1995)</b>	0.19	0.003	0.017	0.002

9



1 **Figure Captions:**



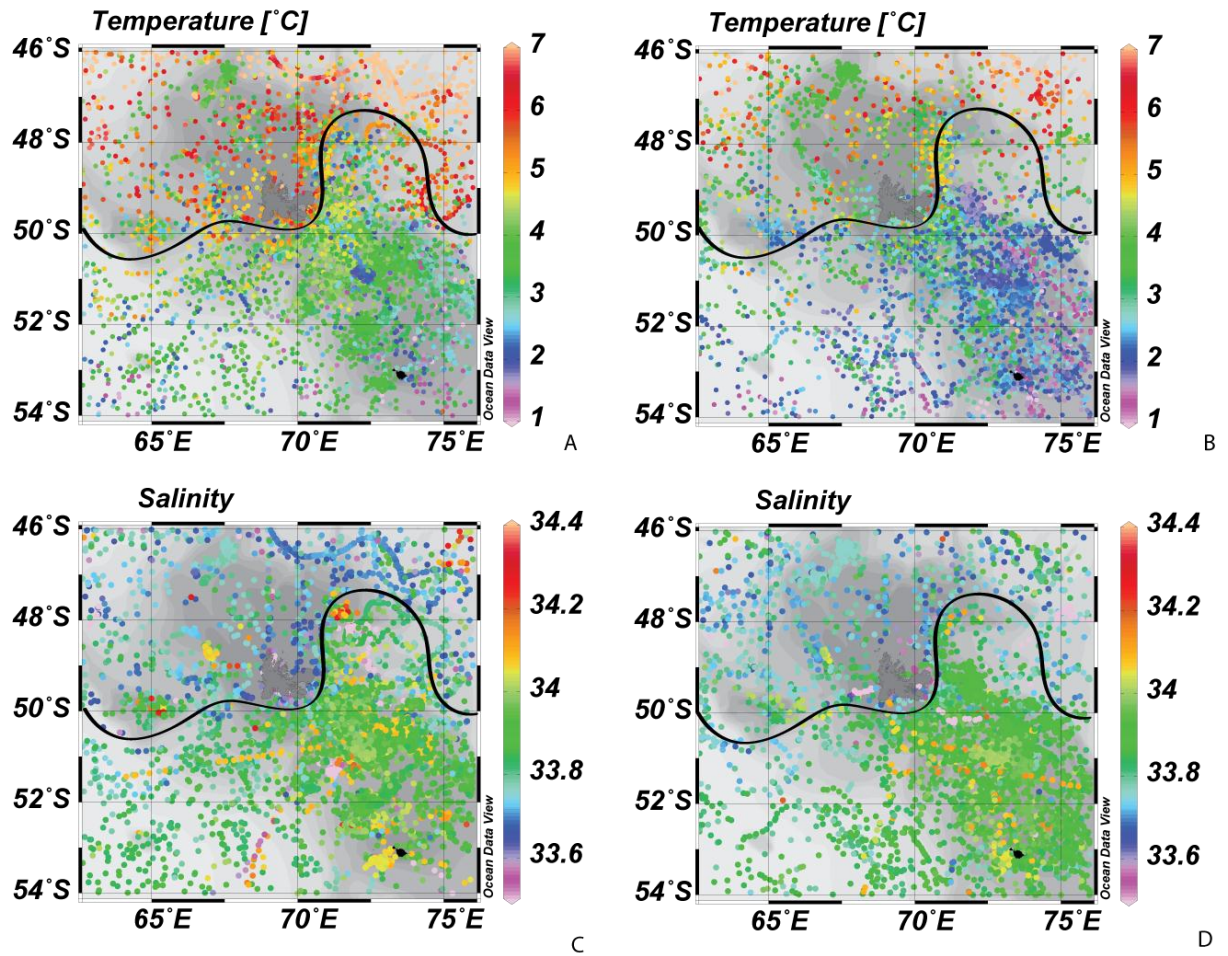
2  
3

4 **Figure 1:**

5 SeaWiFS surface chlorophyll on the 11<sup>th</sup> of November 2011, approximately half way through  
6 the KEOPS2 sampling program. Kerguelen and Heard Island are visible in grey. Stations that  
7 were sampled for suspended particles are indicated with black circles. Distinct regimes of  
8 interest for the KEOPS2 program are indicated in red.

SPRING - SUMMER

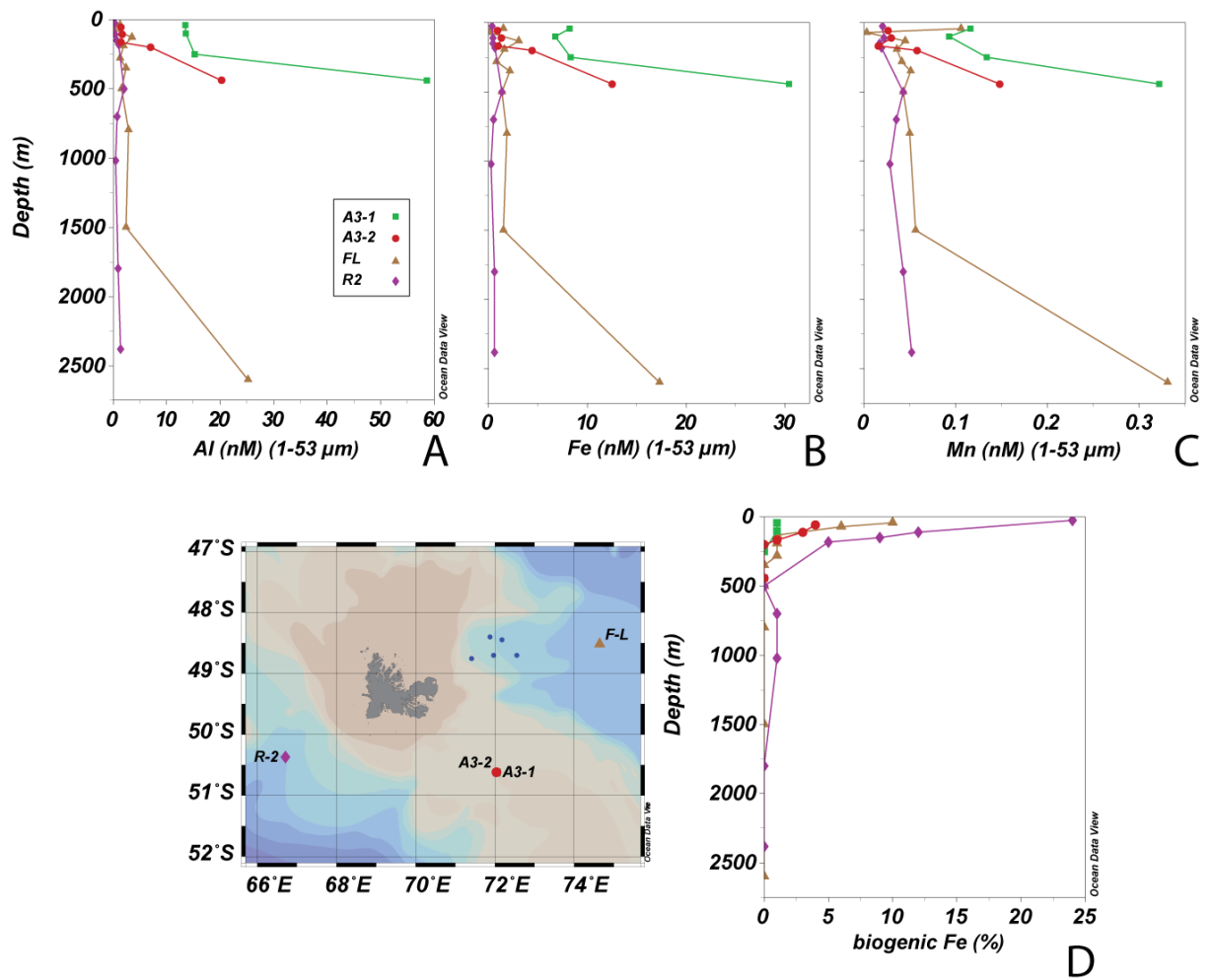
AUTUMN - WINTER



1

2 Figure 2:

3 Surface (10 m) temperature in Spring-Summer (a) and Winter-Autumn (b) as well as surface  
4 salinity in Spring-Summer (c) and Winter-Autumn (d) within the study area from 1970 until  
5 2013. The PF is identified as a solid black line. Kerguelen and Heard Island are visible in dark  
6 grey and black respectively and the Leclaire Rise can be identified as the shallow bathymetry,  
7 north of the PF, near the western boundary of the map. Data obtained from the World Ocean  
8 Database (<http://www.nodc.noaa.gov>).

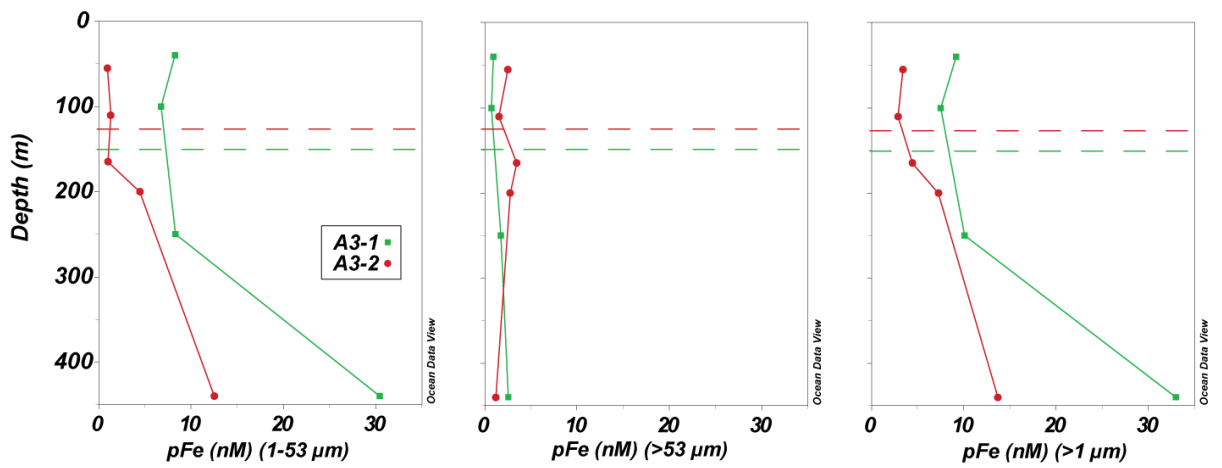


1

2 Figure 3:

3 Profiles of particulate Fe (a), Al (b) and Mn (c) (1 - 53 μm) at the reference HNLC station (R-  
 4 2), the northern PF station (F-L) and pre and post-bloom over the plateau station (A3-1 red  
 5 circle, A3-2 green square), highlighting the contrasting particulate trace metal supply to these  
 6 locations. Biogenic Fe (d) (as a percentage of the total Fe) in surface waters shows a clear  
 7 progression that can be explained by the location of each station within the study area  
 8 whereby, biogenic Fe at R-2 >> F-L > A3-2 > A3-1.





1

2

Figure 4:

3

Particulate Fe at the plateau station (A3) by size class. The integrated full water column pFe

4

(>1μm) reduced by 51% between A3-1 and A3-2 (9.1 – 4.5 mMol m<sup>-2</sup> at A3-1 and A3-2

5

respectively). The integrated mixed layer pFe reduced by 70% between A3-1 and A3-2 (1.4 –

6

0.56 mMol m<sup>-2</sup> at A3-1 and A3-2 respectively). The mixed layer shoaled between A3-1 and

7

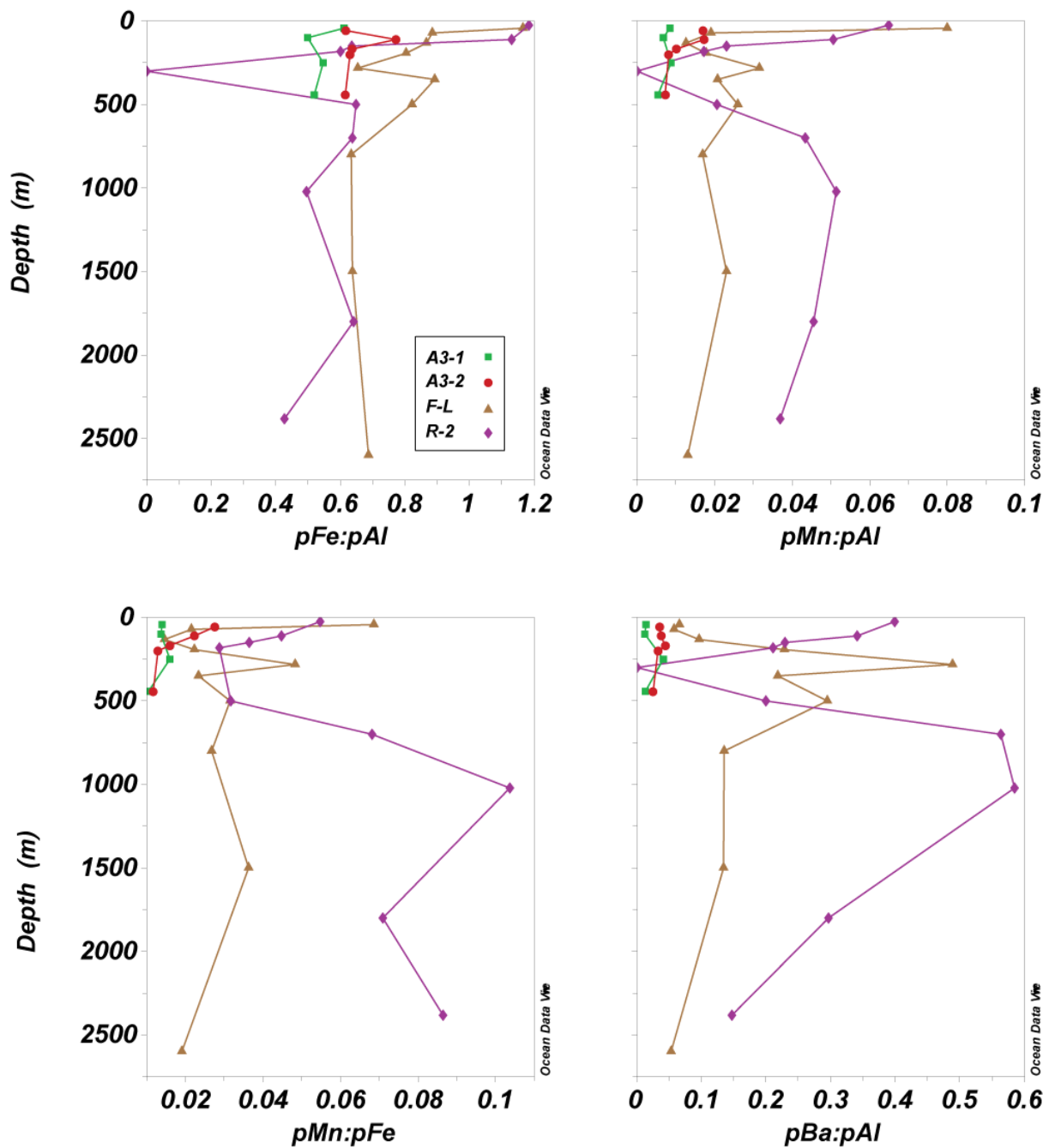
A3-2 as illustrated by the dashed horizontal line. The calculation of integrated mixed layer

8

pFe used a constant mixed layer depth of 165m for both A3-1 and A3-2 to allow comparison

9

between these stations.



1

2

Figure 5:

3

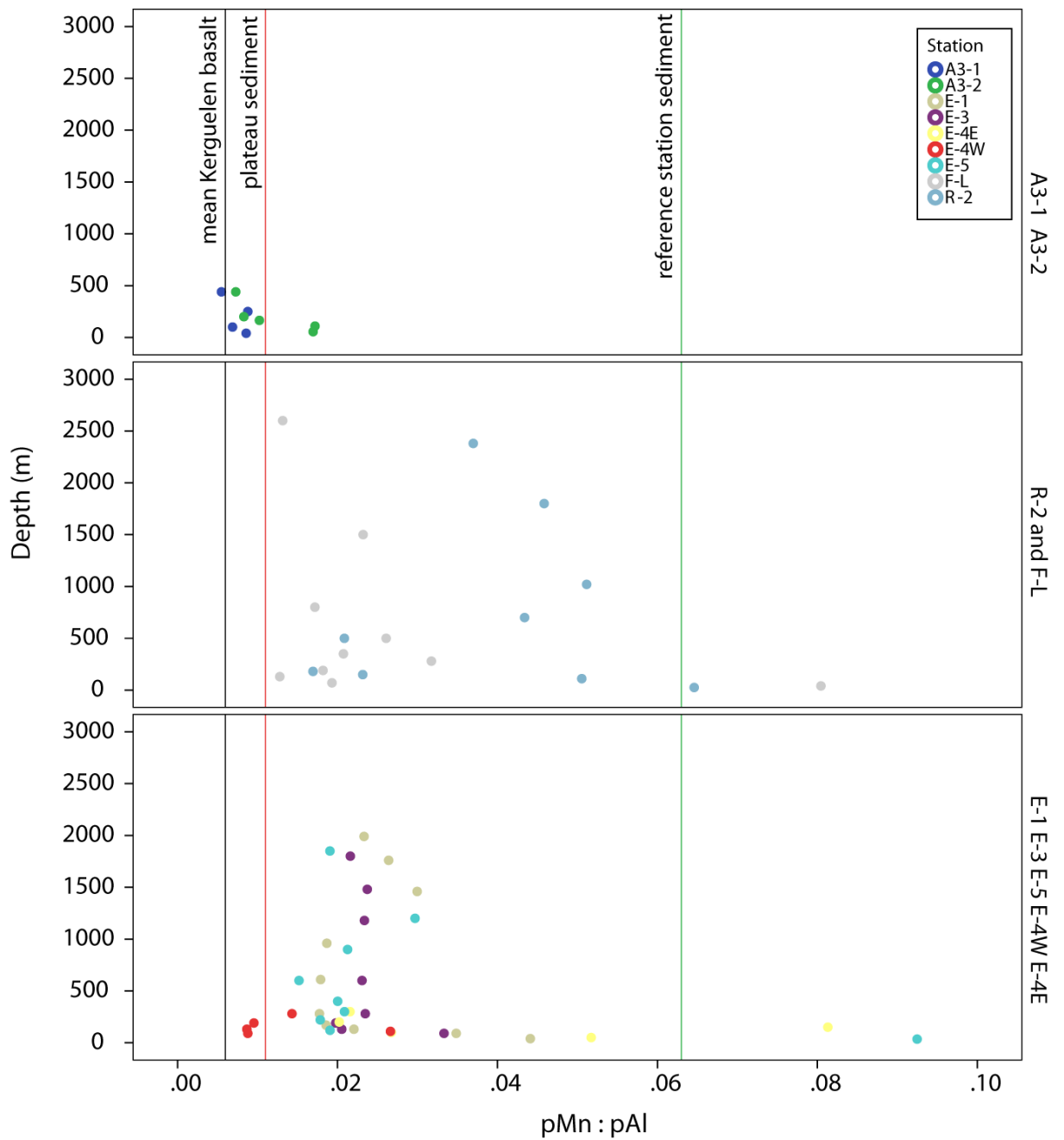
Profiles of elemental ratios at the reference station (R-2), northern PF (F-L) and pre and post-

4

bloom over the plateau station (A3-1, red circles; A3-2, green squares respectively). Note the

5

increase in pMn and pBa relative to pAl at station R-2 below 500 m.



1

2

Figure 6:

3

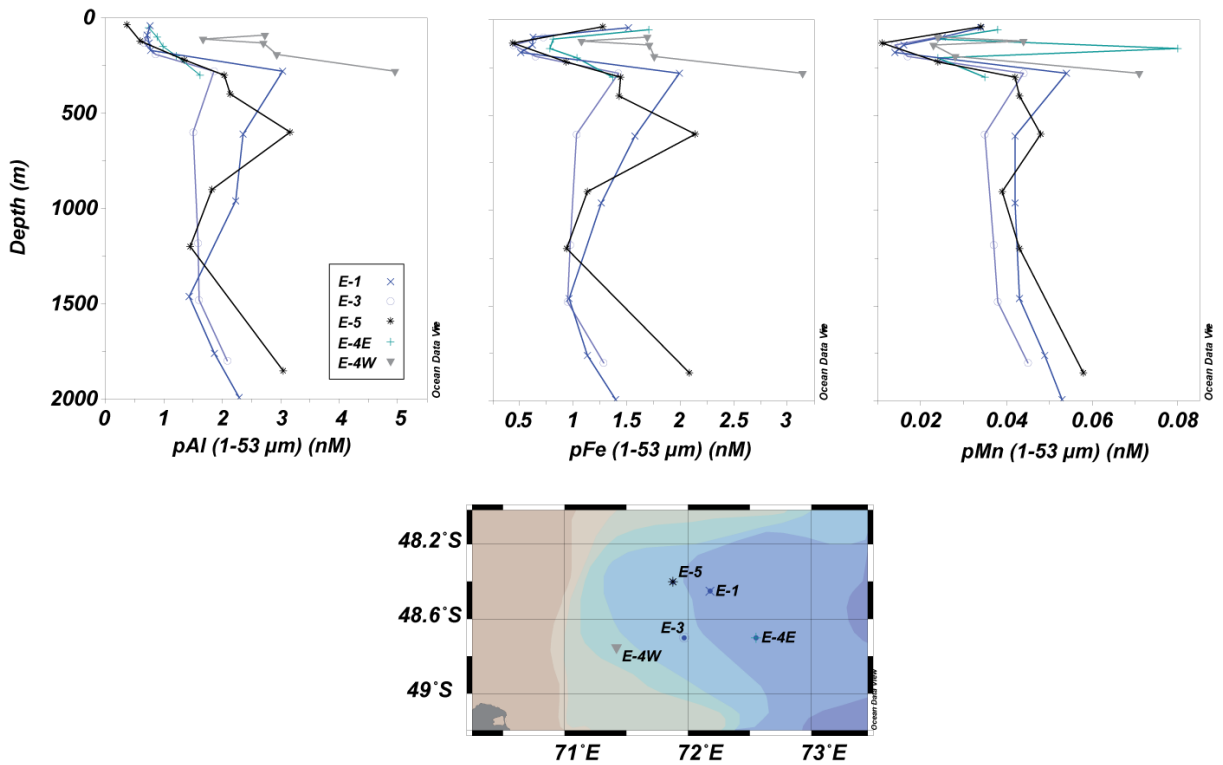
Molar ratio of pMn:pAl versus depth, separated by station type. Vertical lines represent the

4

median molar ratios within Kerguelen Island basalts (Gautier et al., 1990) (black), authigenic

5

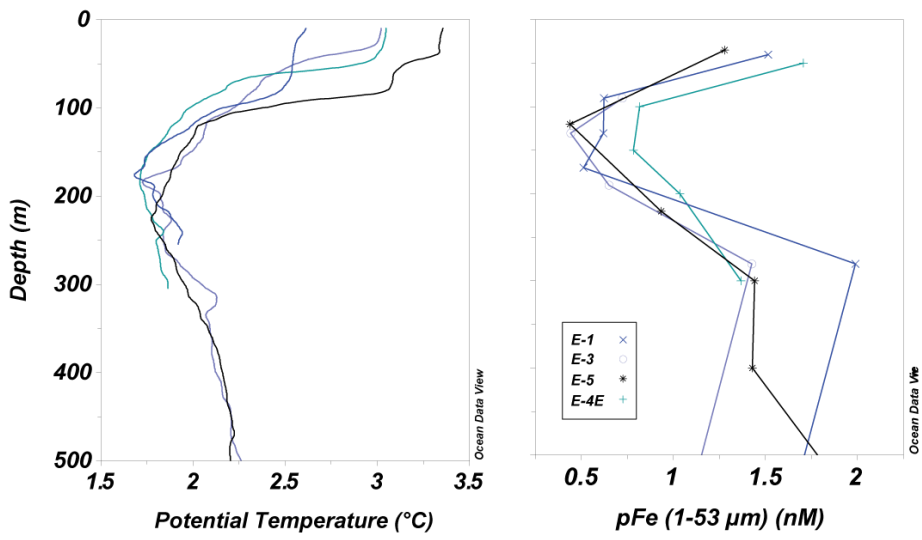
Kerguelen Plateau sediments (red) and station R-2 authigenic sediments (green).



1

2 Figure 7:

3 Profiles of particulate trace metals during the pseudo-lagrangian recirculation-structure study.  
 4 Station E-4W (red circles) exhibits unique trace metal profiles in comparison to the remaining  
 5 stations (see text for details). Note the distinct pFe and pMn minima at 150-175 m. Particulate  
 6 Al exhibits a similar profile albeit without surface enrichment.



7

1            Figure 8:

2        a) Representative temperature profiles within the upper 500 m within the recirculation  
3        structure. b) Particulate Fe (1-53  $\mu\text{m}$ ) within the upper 500 m within the recirculation  
4        structure. Correspondence between the temperature minimum depth of winter water and pFe  
5        minimum is illustrated.

6